

Fabrication and Characterization of Superconducting NbN Nanowire Single Photon Detectors

Jeffrey A. Stern and William H. Farr

Abstract— We report on the fabrication and characterization of high-speed, single photon detectors using superconducting NbN nanowires at a wavelength of 1064 nm. A 15 by 15 microns detector with a detector efficiency of 40% has been measured. Due to kinetic inductance, the recovery time of such large area detectors is longer than that of smaller or single wire detectors. The recovery time of our detectors (50 ns) has been characterized by measuring the inter-arrival time statistics of our detector.

Index Terms— NbN, Single Photon Detector, SNSPD

I. INTRODUCTION

SUPERCONDUCTING, high speed, single-photon detectors at optical and near infrared wavelengths have application in optical communication, quantum optics and semiconductor chip analysis. These detectors use a small (5 nm thick by 10 nm wide) NbN wire, which is biased just below the superconducting critical current of the wire. When a photon strikes the wire, a large number ($\approx 10^3$) excited electrons are formed, locally depressing the critical current of the wire. As the bias current exceeds the critical current, the hot-spot rapidly goes normal causing the current to drop and a voltage signal pulse. The electron-phonon recombination time in NbN is short, so the hot spot rapidly dissipates. In a typical detector, the NbN wire is formed into a meander which fills a rectangular pixel to increase the collecting area.

Superconducting Nanowire Single Photon Detectors (SNSPDs) were first reported on by Kadin *et al.* [1], and first implemented in NbN by Gol'tsman *et al.* [2]. More recently Rosfjord *et al.* [3] have demonstrated high detector efficiency (DE, 67% at 1064 nm) with small ($3.3 \times 3.0 \mu\text{m}^2$) pixels. However, recent measurements and theory indicate that the kinetic inductance (KI) of the meander limits the recovery time of these detectors, and that this recovery time is proportional to the wire length divided by its cross-section [4]. In this work we discuss our fabrication process and the properties of SNSPDs with pixel sizes that are large enough ($15 \times 15 \mu\text{m}^2$) to efficiently couple to a 1064 fiber optic waveguide.

II. FABRICATION

A. NbN Deposition

NbN films for SNSPDs were deposited on both c-axis quartz and sapphire. These materials were chosen because they had good thermal conduction, and uniform index of refraction. Previous SNSPDs have been fabricated on r-plane sapphire, which is not homogenous. Optical signals, which are backside coupled into these devices, will have their polarization rotated, which may be an issue in some applications. Our substrate heater uses direct absorption of light from quartz lamps; prior to final wafer cleaning, we deposit 100 nm of Nb on the backside of our wafers as an absorber. The substrates are then ultrasonically cleaned in a series of solvents (detergent, deionized water, acetone, propanol and again in deionized water.) The sample is then dried and introduced into the vacuum system through a load lock chamber.

All NbN films were deposited at JPL using reactive, DC magnetron sputtering from a Nb target in an Ar-N₂ gas mixture. The deposition process is similar to that used for NbTiN hot-electron bolometers [5]. The vacuum chamber has a typical base pressure of 4×10^{-7} Pa. The samples are in-situ, Argon-ion cleaned by applying an RF bias to the substrate. The typical thickness for this work was 27 nm. The substrate is then heated to 500-600° C as measured by a thermocouple touching the back of the sample. The NbN film is deposited with an RF bias applied to the substrate to induce a DC voltage of 40-70 V. This RF bias promotes a dense, smooth film by increasing the surface energy of the ions on the film surface. The gas mixer is controlled by mass-flow controllers to be 150 sccm of Ar and 18 sccm of N₂. The cryo-pump is then throttled to maintain a pressure of 0.93 Pa. The NbN films are typically deposited at 1.00 A and -240 V.

B. SNSPD Fabrication

Sample fabrication is very similar to that described by Gol'tsman *et al.* [6] and Yang *et al.* [7]. The meanders are fabricated on the front side of the quartz (or sapphire) wafer, and the radiation is coupled in through the substrate. The

Manuscript received August 28, 2006. This work was supported by NASAs Space Mission Directorate.

J. A. Stern is with the Jet Propulsion Laboratory, MS 302-231, Pasadena, CA 91109 USA (818-354-0029; fax: 818-393-4663; e-mail: stern@jpl.nasa.gov).

W. H. Farr is with the Jet Propulsion Laboratory, MS 161-135, Pasadena, CA 91109 USA (818-354-1989; fax: 818-393-6142; e-mail: william.h.farr@jpl.nasa.gov).

devices tested in this paper used poly methyl methacrylate (pmma) e-beam resist. This process will be described in detail. More recently, we are using a hydrogen silsesquioxane (HSQ) resist similar to that described by Yang. The HSQ process is less complex and yields better uniformity. Figure 1 shows an SEM image of a recent device processed using HSQ prior to the NbN etch and cavity deposition. These devices have not yet been measured optically.

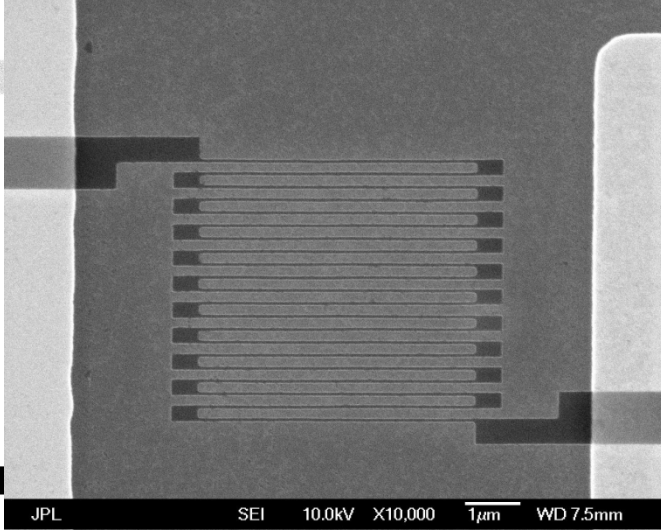


Fig. 1. SEM image of a $5 \times 5 \mu\text{m}^2$ SNSPD. The wires are 80 nm wide on a 240 nm spacing.

Prior to fabricating the device, the NbN film is protected with a photoresist coating, and the Nb layer on the backside of the wafer is removed by reactive ion etching (RIE). Next, a wire layer (Ti—1.5 nm/Au—80 nm) is deposited using a photoresist liftoff-stencil. To ensure good electrical contact between the NbN and the Ti-Au wiring layer, the sample is in-situ cleaned using a Kauffman type ion mill. The gold wire layer forms a co-planer waveguide circuit for the high frequency electrical output and DC bias.

The NbN wire is formed with a series of two etches. First, the wafer is coated with pmma. The gaps between the wires are then exposed in a JEOL field-emission lithography system at 100 keV accelerator voltage. The exposed pmma is developed out in methyl-isobutyl-ketone mixed with isopropanol, and the wafer is etched in an inductively coupled plasma etcher using SF_6 . This first etch removes the material between the NbN wires, but leaves the NbN over most of the wafer. The SF_6 ICP etched NbN very quickly. To better control the etch times, subsequent SNSPD wafers were processed with an SF_6 reactive ion etch at low pressure and power.

The second etch is masked by a two layer stack of SiO and Al. This bi-layer acts as both the etch mask and the dielectric cavity for the SNSPD. The SiO layer is 135 nm, which was picked to be a quarter-wavelength at 1064 nm. The Al layer is 50 nm thick and acts as a reflective layer. The bi-layer is deposited by thermal (SiO) and electron-beam (Au) evaporation through a liftoff stencil. Figure 2 shows an optical

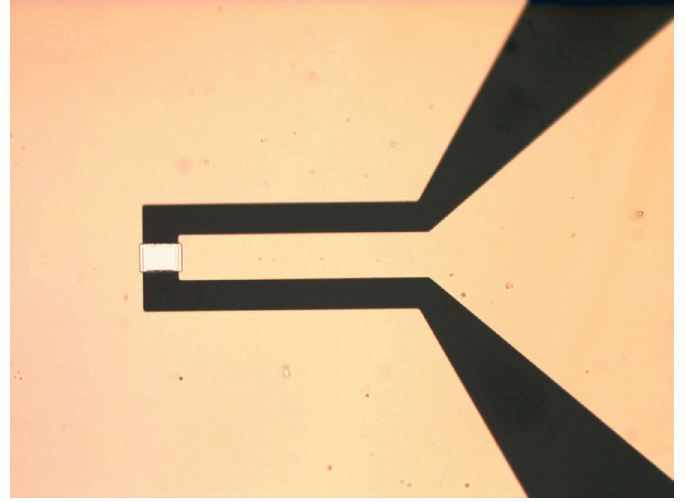


Fig. 2. Optical micrograph of a $10 \times 10 \mu\text{m}^2$ SNSPD. The gold CPW transmission line is visible with the Al reflector covering the actual detector.

micrograph of a completed device. In some experiments we front-side coupled through the SiO layer, by first removing the Al layer in a weak basic solution. For longer wavelengths it is advantageous to replace the Al with a Au or Ag reflector. The remaining NbN was removed in a second SF_6 etch. The backside of the quartz substrate was not anti-reflection coated,

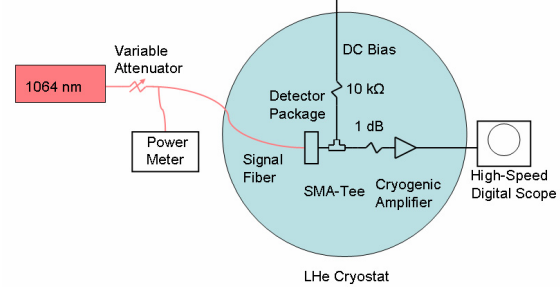


Fig. 3. Experimental apparatus for measuring SNSPD chips

so there was 5% reflection loss at this interface.

III. EXPERIMENTAL SETUP

All measurements were done in an infrared systems, 8-inch diameter cryostat. Figure 3 shows a schematic of the test apparatus. The SNSPD chip was mounted into a microwave package, and wire bonded to either a series chip resistor or a 1 dB chip attenuator. The resistor/attenuator was then bonded to the center conductor of the microwave connector. The use of a chip resistor and later the 1 dB chip attenuator was important in achieving a stable electrical bias of the SNSPD and to attenuate internal reflections from the preamplifier. The chip package was clamped to the cold plate of the dewar using indium foil, and it was connected to an AC coupled cryogenic

preamp through a simple tee connector. The output of the preamp was connected directly to the high-speed digital oscilloscope.

The optical source was an attenuated, continuous, 1064 nm laser to approximate a Poisson source. The output power of the laser was monitored through a calibrated 3dB splitter and measured with a calibrated power meter. For the DE measurements, the output of the single mode fiber was collimated and passed through a calibrated 2.1 mm diameter aperture. The total power through the aperture was measured to get an accurate optical flux density, and the detector was then over illuminated, and the flux on the detector determined to be the optical flux density times the detector area ($15 \times 15 \mu\text{m}^2$).

IV. RESULTS AND DISCUSSION

A. Detector Efficiency Measurement

The optical detection efficiency was measured on a $15 \times 15 \mu\text{m}^2$ SNSPD with 120 nm wide wires on 240 nm spacing. The critical current of this meander was approximately 12 μA . The detector was measured twice. The first time the detector was illuminated from the backside with the Al reflector in place. For the second measurement, the Al layer was etched off in a weak base, and the optical signal was coupled in from the front side of the wafer. For both measurements, we pumped on the He cryostat to get below 4.2 K, however, our pump was not large enough to get below 3.1 K. For these measurements, the bias current was set as high as was stable. As the temperature is reduced, the bias current is increased.

The data for the detector efficiency (DE) measurements is shown in Figure 4. In all of the measurements, the dark counts were subtracted out prior to calculating the DE. For the lowest temperature (3.1 K) and the highest bias current (12.5 μA) a detector efficiency of $40.2 \pm 1.8\%$ was achieved for the backside coupled device. For similar bias/temperature conditions, the backside device had a DE that was 50% higher

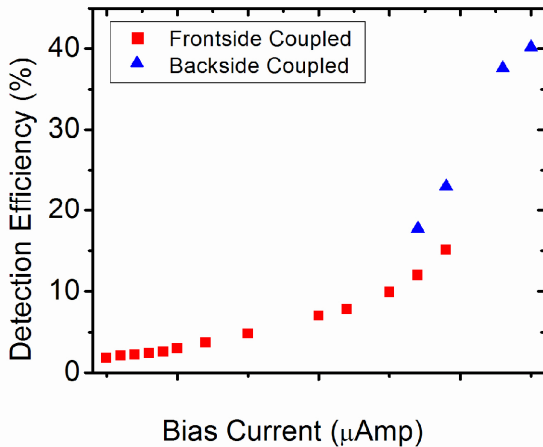


Fig. 4. Detector efficiency as a function of bias current for both a device coupled through the backside and frontside of the wafer. With increasing bias current the corresponding temperature is decreasing from 3.8 to 3.1 K (left side of plot to right).

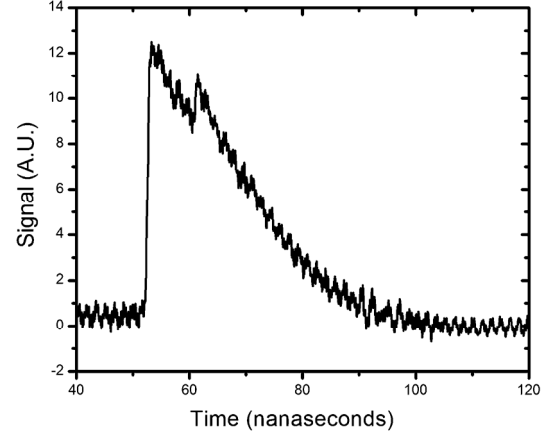


Fig. 5. Response of a $15 \times 15 \mu\text{m}^2$ SNSPD to a 1064 nm photon. The rise time is 200 ps and the fall time 15 ns.

than the frontside device. At the lowest two temperatures, the detector efficiency is flattening out. We anticipate that it would saturate somewhere between 3 and 2 K. The dark count rate for the 40% DE data was 27 kHz.

B. Recovery Time Measurements

Figure 5 shows the digitized output signal in response to 1064 nm radiation. The rise time for the detector is quite fast (200 ps), while the fall time is substantially longer (15 ns). Because the DE of the SNSPD is a strong nonlinear function of the bias current, the DE will recover is an even longer time [4]. A very accurate method of measuring the recovery time for the detector is by studying the statistics of the interarrival time for photons. Figure 6 shows the photon arrival rate (on a log scale) after an initial photon triggers the scope for a 5 by 5 μm^2

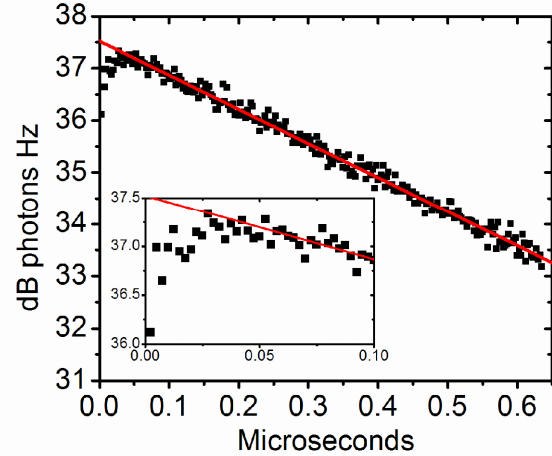


Fig. 6. The photon arrival rate as a function of pulse separation (interarrival time) for a $5 \times 5 \mu\text{m}^2$ SNSPD. The red line is a fit to the data above 100 ns. The inset shows the 1 dB of DE suppression at 5 ns.

μm^2 meander. The NbN wire is 12 nm and the spacing 24 nm. For a true Poisson distribution, this curve should be a straight line; however, we see 1 dB of DE suppression for up to 5 ns, which, if you factor in the detector dimensions, is in

agreement with Kerman [4].

V. CONCLUSIONS AND FUTURE WORK

We have successfully fabricated large area, high DE SNSPDs with NbN films grown at JPL. We anticipate that the DE can be increased further by slightly lowering the operating temperature, improving the uniformity of our NbN wires, optimizing our dielectric cavity, and anti-reflection coating the backside of our wafer. The DE's achieved here and by others are sufficiently high to support many applications. However, to take advantage of these detectors, the recovery times must be improved. We believe the best approach to this problem is to manufacture arrays of smaller SNSPD detectors. This improves the speed of these detectors in two ways. First, smaller individual pixels will have lower KI, and thus shorter recovery times. Second, in a low flux environment, the probability of a second photon striking an individual pixel during the recovery time, can be made small if the number of pixels is large. The challenge of implementing these arrays will be improving the uniformity and yield of the SNSPDs, and implementing a low noise readout scheme that is compatible with the low temperature operation of these devices.

ACKNOWLEDGMENT

The Authors wish to acknowledge Richard Muller for operating the e-beam lithography tool, Sae Woo Nam and Karl Berggren for useful discussions on SNSPDs, and Gregory Gol'tsman for useful discussions on the deposition of thin NbN films.

REFERENCES

- [1] A. M. Kadin and M. W. Johnson, "Nonequilibrium photon-induced hotspot: A new mechanism for photodetection in ultrathin metallic films," *Appl. Phys. Lett.* **69**, ppp. 3938-3940, 1996.
- [2] G. Gol'tsman, *et al.*, "Picosecond superconducting single-photon optical detectors," *Appl. Phys. Lett.* **79**, pp. 705-707, 2001.
- [3] K. M. Rosfjord, *et al.*, "Nanowire Single-Photon Detector with an Integrated Optical Cavity and Anti-Reflection Coating," *Opt. Express*, pp. 527-534 2006.
- [4] A. J. Kerman *et al.*, "Kinetic-inductance-limited reset time of superconducting nanowire photon counters," *Appl. Phys. Lett.* **88**, pp. 111116, 2006.
- [5] J. A. Stern, B. Bumble, J. Kawamura and A. Sklare, "Fabrication of Terahertz Frequency Phonon Cooled HEB Mixers," *IEEE Trans. Appl. Supercond.* **15**, pp. 499-502, 2005
- [6] J. K. W. Yang *et al.*, "Fabrication Development for Nanowire GHz-Counting-Rate Single-Photon Detectors," *IEEE Trans. Appl. Supercond.* **15**, pp. 626-629, 2005.
- [7] G. Gol'tsman *et al.*, "Fabrication and properties of an ultrafast NbN hot-electron single-photon detector," *IEEE Trans Appl. Supercond.* **11**, pp. 574-577, 2001.